

# Probing Left-handed Heavy Neutral Leptons in the Vector Scotogenic Model

Paulo Areyuna C.<sup>1,3,\*</sup> Jilberto Zamora-Saa<sup>2,3,†</sup> and Alfonso R. Zerwekh<sup>1,3,4‡</sup>

<sup>1</sup> *Universidad Técnica Federico Santa María Casilla 110-V, Valparaíso, Chile.*

<sup>2</sup> *Center for Theoretical and Experimental Particle Physics - CTEPP,*

*Facultad de Ciencias Exactas, Universidad Andres Bello,*

*Fernandez Concha 700, Santiago, Chile.*

<sup>3</sup> *Millennium Institute for Subatomic physics at high energy frontier - SAPHIR,*

*Fernandez Concha 700, Santiago, Chile. and*

<sup>4</sup> *Centro Científico - Tecnológico de Valparaíso, Casilla 110-V, Valparaíso, Chile*

In this work, we consider an extension to the Standard Model composed by a Massive Vector Doublet under  $SU(2)_L$  and a Left-handed Heavy Neutral Lepton. We study the production of these exotic leptons with the Same Flavor Opposite Sign standard lepton pair, and jets, considering Drell-Yan and Vector Boson Fusion as independent cases. We find that for the latter, the dilepton angular distribution is different enough from the background to use it as a smoking-gun for our model. Based on this fact, we establish limits on the parameter space considering previous experimental searches in this final state.

Keywords: Left-handed Heavy Neutral Lepton, Left-handed Heavy Neutrinos, Massive Vector Doublet Model, ATLAS experiment.

---

\* paulo.areyuna@sansano.usm.cl

† jilberto.zamora@unab.cl; jilberto.zamorasaa@cern.ch

‡ alfonso.zerwekh@usm.cl

## I. INTRODUCTION

The standard model of particle physics (SM) is the most complete and successful explanation of the fundamental interactions. Despite its awesome phenomenological achievements, this model is not able to explain all the observed phenomena. Among them we can mention, for example, the presence of Dark Matter (DM) in the universe. Although we know very well the amount of DM in the Universe (in terms of relic density) [1], we know nothing about its nature.

Another problem is the neutrino mass generation mechanism. Due to the apparent absence of right-handed neutrinos, it is impossible to generate neutrino masses through Yukawa couplings as the other fermions do. Moreover, even if right handed neutrinos exist, the Yukawa coupling needed to explain the neutrino masses would be so small that the standard mechanism for mass generation seems to be unnatural for the neutrinos. In this context, it would be of great interest if these two apparently independent problems (dark matter and neutrino mass generation) could be connected. Part of the aim of this work is to propose a mechanism for studying one realization of this intriguing possibility.

Among the variety of proposed ideas that may describe the physics of dark matter, the minimal dark matter program [2] appears as specially appealing. Initially, it was developed for scalar and fermion fields. However, it was later shown that the mechanism worked very well also for vector fields. In reference [3], for instance, it was shown that the inclusion of a new massive field in the adjoint representation of  $SU(2)_L$  provide a viable dark matter candidate. Additionally, the case of a massive vector field in the fundamental representation of  $SU(2)_L$  was also successfully studied in reference [4]. Interestingly enough, this last model can be naturally extended by the inclusion of a sterile left-handed heavy neutral lepton (HNL) [5]. In this version, the model is capable of solving both problems: dark matter and neutrino mass generation mechanism [4–6]. Indeed, this model has been shown to be able of tackling also the muon  $(g - 2)$  problem [6].

In this work, we perform a phenomenological study for the production of these new particles (*i.e.* the new massive vector boson and the left-handed HNL) in the Large Hadron Collider (LHC). We use existing experimental data to constrain the model parameters, as a function of the sensitivity of current experiments. Additionally, we make predictions based on the kinematical features of the production process, in order to facilitate the search of

these new particles in future measurements.

The paper is organized as follows: In Section II we describe the main features of the proposed model, while in Section III we discuss the main production mechanisms of these new particles at the LHC. In Sections IV and V we study the production mechanisms in order to define upper limits on the parameter space, and focus on the kinematical signatures of each process. In Section VI we study the discovery potential of the model at future experimental facilities, and in Section VII we obtain an estimation of lower limits for the parameter space coming from dark matter measurements. Finally, our conclusions are presented in Section VIII.

## II. THEORETICAL BACKGROUND

Let us start by introducing the following set of vectors:

$$V_\mu = \begin{pmatrix} V_\mu^+ \\ V_\mu^0 \end{pmatrix} = \begin{pmatrix} V_\mu^+ \\ \frac{1}{\sqrt{2}}(V_\mu^1 + iV_\mu^2) \end{pmatrix}, \quad (1)$$

which transforms as  $(1, 2, 1/2)$  under the SM group  $SU(3)_c \times SU(2)_L \times U(1)_Y$ . The dynamics of this new vector doublet is described by the following lagrangian:

$$\begin{aligned} \mathcal{L} = \mathcal{L}_{SM} &- \frac{1}{2}(D_\mu V_\nu - D_\nu V_\mu)^\dagger (D^\mu V^\nu - D^\nu V^\mu) + i\frac{g'\kappa_1}{2}V_\mu^\dagger B^{\mu\nu}V_\nu + ig\kappa_2 V_\mu^\dagger W^{\mu\nu}V_\nu \\ &+ M_V^2 V_\mu^\dagger V^\mu - \alpha_2(V_\mu^\dagger V^\mu)(V_\nu^\dagger V^\nu) - \alpha_3(V_\mu^\dagger V^\nu)(V_\nu^\dagger V^\mu) \\ &- \lambda_2(\Phi^\dagger \Phi)(V_\mu^\dagger V^\mu) - \lambda_3(\Phi^\dagger V_\mu)(V^{\mu\dagger} \Phi) - \frac{\lambda_4}{2}[(\Phi^\dagger V_\mu)(\Phi^\dagger V^\mu) + (V^{\mu\dagger} \Phi)(V_\mu^\dagger \Phi)], \end{aligned} \quad (2)$$

where  $D_\mu$  stands for the covariant derivative,  $W^{\mu\nu}$  and  $B^{\mu\nu}$  are the field strengths of  $SU(2)_L$  and  $U(1)_Y$ , respectively, and  $\Phi$  is the SM Higgs doublet. This lagrangian was labeled by the authors as the Vector Doublet Dark Matter Model (VDDMM), since the neutral component of the vector has been proven to account for DM (see reference [4]). It's worth to mention the presence of non minimal gauge interactions. The coupling constants associated to these interactions ( $\kappa_1$  and  $\kappa_2$ ) are free parameters. In reference [4] the authors set their values as  $\kappa_1 = \kappa_2 = 1$ , in order to avoid interactions between the photons and the neutral component of the vector doublet. This restriction can be full filled with a more general condition:  $\kappa_1 = \kappa_2 = \kappa$ . However, since the phenomenology of the model has been studied with  $\kappa = 1$ , we are going to keep this choice, despite the fact that a different choice of this value can

produce an interesting phenomenology. Additionally, the lagrangian presents an accidental  $Z_2$  symmetry, making the lightest neutral vector as a viable DM candidate.

In order to perform calculations, it's useful to define some quantities after the symmetry breaking:

$$\begin{aligned}
M_{V^\pm}^2 &= \frac{1}{2}(2M_V^2 - v^2\lambda_2) \\
M_{V^1}^2 &= \frac{1}{2}(2M_V^2 - v^2[\lambda_2 + \lambda_3 + \lambda_4]) \\
M_{V^2}^2 &= \frac{1}{2}(2M_V^2 - v^2[\lambda_2 + \lambda_3 - \lambda_4]) \\
\lambda_L &= \lambda_2 + \lambda_3 + \lambda_4.
\end{aligned} \tag{3}$$

The latter is the coupling that describes the interaction between the Higgs boson and  $V^1$ . Moreover, in this work, we are particularly interested on the production of these vector states, therefore, we don't need to pay attention on the quartic interactions, having in consequence only 4 relevant parameters. For convenience, we perform a change of basis for them, and write the lagrangian in terms of the previously presented parameters:

$$\begin{aligned}
\lambda_2 &= \lambda_L + 2\frac{M_{V^1}^2 - M_{V^\pm}^2}{v^2} \\
\lambda_3 &= \frac{2M_{V^\pm}^2 - M_{V^1}^2 - M_{V^2}^2}{v^2} \\
\lambda_4 &= \frac{M_{V^2}^2 - M_{V^1}^2}{v^2} \\
M_V^2 &= M_{V^1}^2 + \frac{v^2}{2}\lambda_L.
\end{aligned} \tag{4}$$

Henceforth, we are going to consider the special case of  $M_{V^1} = M_{V^2} \equiv M_{V^0}$ . This special case is motivated by the results obtained in reference [4]. In addition, we define the quantity  $\Delta M = M_{V^+} - M_{V^0}$ .

Due to the vector doublet quantum numbers and Lorentz invariance, it is not possible to link directly the new vector field to the SM fermions. However, if we introduce an exotic left-handed neutrino which is singlet of the SM, we can write the following interaction term:

$$\mathcal{L}_{VNL} = - \sum_{k=\{e,\mu,\tau\}} \beta_k \bar{L}_k \gamma^\mu \tilde{V}_\mu N_L + \text{h.c.} , \tag{5}$$

with

$$\tilde{V}_\mu = i\sigma_2 V_\mu^* = \begin{pmatrix} \frac{1}{\sqrt{2}}(V_\mu^1 - iV_\mu^2) \\ -V_\mu^- \end{pmatrix} . \tag{6}$$

In Eq. 5,  $N_L$  stands for a left-handed Majorana fermion with definite mass  $M_N$ , which acts as a portal between the vector doublet and SM leptons. If we define  $N_L$  as  $Z_2$  odd, the accidental symmetry is respected, and this new fermion can also be a DM candidate, depending if it's lighter than the vector candidate. The addition of a new fermion state allows the generation of radiative neutrino masses (see Figure 1). The necessary conditions for reproducing the neutrino mixing matrix have been studied with two [5] and three [6] HNLs. Since the scope of the present work is focused on determining the detection prospects of the model at the LHC, we will work with just one HNL. This simplifying assumption allows us to explore different values of the  $\beta$  couplings without concerning about neutrino mass generation, because it is always possible to attribute the neutrino mass generation to extra HNLs with masses beyond LHC sensitivity. Due to the similarities between the scotogenic model proposed by Ma in reference [7] and our construction, we will refer to the model treated in this work as the Vector Scotogenic Model.

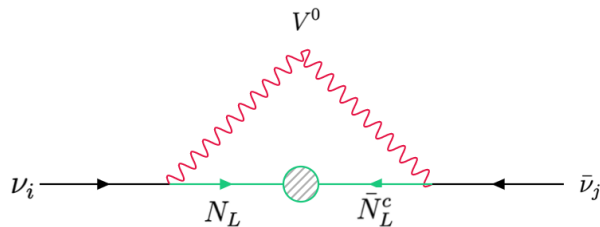


FIG. 1: Neutrino mass generation mechanism in the Vector Scotogenic Model.

### III. PRODUCTION MECHANISM AT THE LHC

As we stated above, we are interested in the study of the Vector Scotogenic model in the context of LHC, particularly at the ATLAS detector. The signal to be searched is composed by two HNL in the final state, which can be used as smoking gun of this new physics. These fermions can be produced mainly in two type of processes: Drell-Yan (DY) and Vector Boson Fusion (VBF) as can be seen in Figure 2. The main difference between these mechanisms is the presence of jets in the final state of VBF.

We used FeynRules [8–10] to obtain the Feynman rules for the new sector, and Madgraph5\_aMC@NLO version 3.5.0 [11] to compute the cross section for these processes at  $\sqrt{s} = 13$  [TeV], considering all the possible diagrams. It's worth mentioning that the pro-

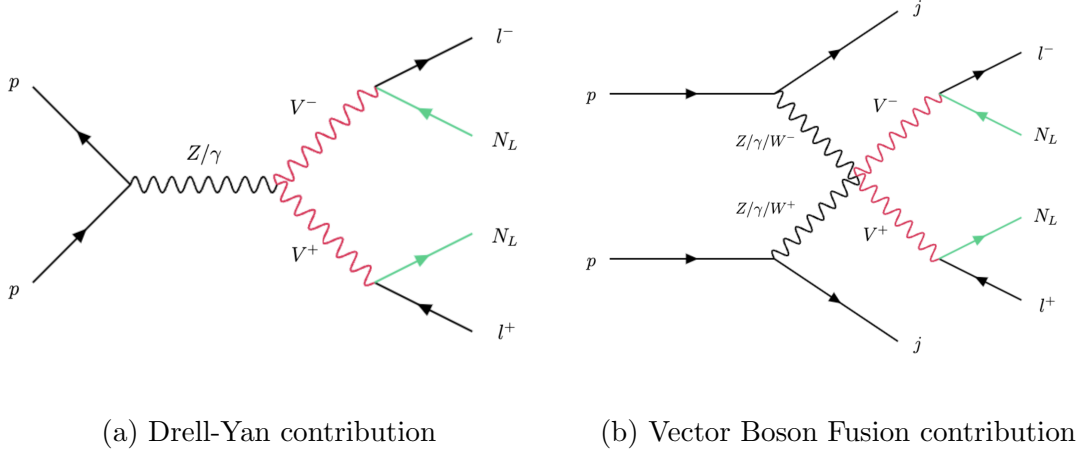


FIG. 2: Production mechanisms at the LHC.

duction process depends strongly on the charged vector decay width. Since we are restricted to the completely degenerate scenario, the only decay channel is through the trilinear term in eq. (5). Then, neglecting the lepton masses, this quantity can be written as follows

$$\Gamma_{V^+} = (|\beta_e|^2 + |\beta_\mu|^2 + |\beta_\tau|^2) \frac{(M_{V^+}^2 - M_N^2)^2 (2M_{V^+}^2 + M_N^2)}{(48\pi M_{V^+}^5)}. \quad (7)$$

We have performed our analysis for different values of  $M_{V^+}$  and  $\beta_\mu$ , restricting ourselves to the degenerate case where  $\Delta M = 0$ . As a first step, we have considered only muons in the final state. The study was carried out considering fixed values for the remaining parameters, presented in Table I. The choice of the  $\beta$  couplings has been motivated by the strong constraints on Lepton Flavor Violating decays.

	$M_N$	$\beta_e$	$\beta_\tau$	$\lambda_L$
BP1	50[GeV]	0	0.5	5
BP2	50[GeV]	0	1	5

TABLE I: Benchmark values for the fixed parameters.

Additionally, we have simulated the SM background for each type of the studied processes at  $\sqrt{s} = 13$  [TeV]:  $pp \rightarrow \mu^+ \mu^- \bar{\nu} \nu$  for DY and  $pp \rightarrow jj \mu^+ \mu^- \bar{\nu} \nu$  for VBF (notice that in both cases the neutrinos can be of any flavour).

Firstly, we have computed the cross section for each process without considering kinematical cuts and the detector efficiency, as can be seen in Table II. Here, we have found that

DY cross sections dominate by one order of magnitude over VBF. In addition, the current experimental limits for DY production of new physics are stronger. Therefore, due to the aforementioned, we will focus only on the DY type to set upper-bounds.

It's worth mentioning that for both types of processes, we need to compute the effective cross section  $\sigma_{eff}$ , defined as

$$\sigma_{eff} = \epsilon \mathcal{A} \sigma, \quad (8)$$

where  $\epsilon$  stands for the detector efficiency and  $\mathcal{A}$  represents the acceptance, defined as the ratio of the number of events satisfying the event selection criteria and the total number of selected events. A naive guess is to consider  $\epsilon = 0.55$ , motivated by the efficiency of muon reconstruction [12], however, we consider two scenarios:  $\epsilon = 0.2$  and  $\epsilon = 0.55$  (The choice of the first value is well motivated by the results in Appendix A). On the other hand, the acceptance must be computed for each simulated sample, which must be done separately because the processes have different event selection criteria.

	$M_{V+} = 200[\text{GeV}]$	$M_{V+} = 500[\text{GeV}]$	$M_{V+} = 800[\text{GeV}]$	ATLAS upper limit
$\sigma_{DY}[\text{fb}]$	$1.74 \times 10^{-4}$	$1.32 \times 10^{-6}$	$6.56 \times 10^{-8}$	0.25 [13]
$\sigma_{VBF}[\text{fb}]$	$7.86 \times 10^{-5}$	$2.06 \times 10^{-7}$	$7.89 \times 10^{-9}$	2.67 [14]

TABLE II: Benchmark values for the production cross section, for BP1 and a fixed value of

$$\beta_{\mu} = 0.01.$$

#### IV. DRELL-YAN PRODUCTION

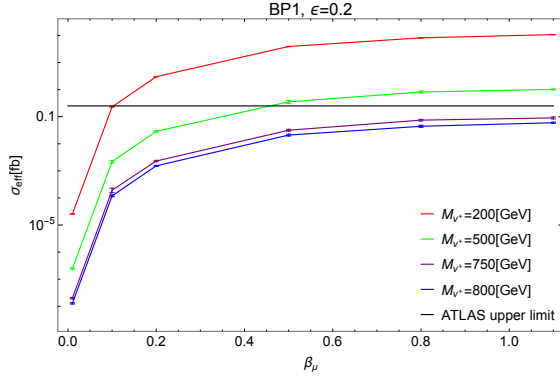
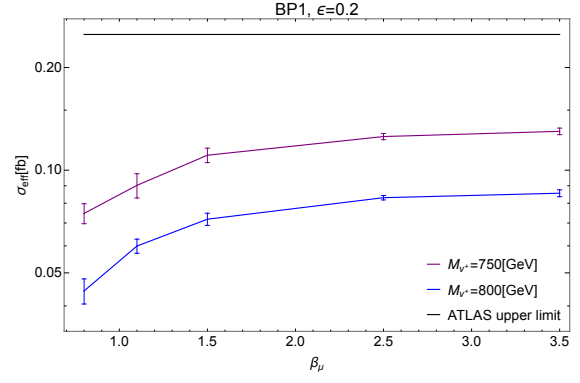
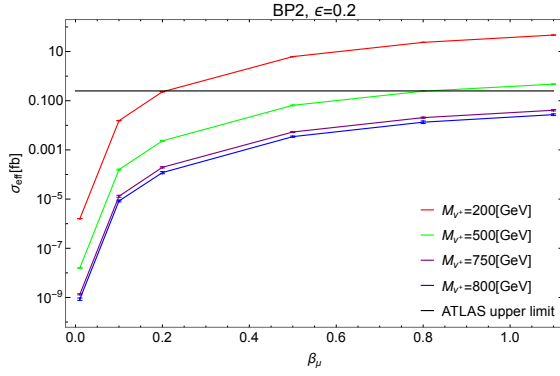
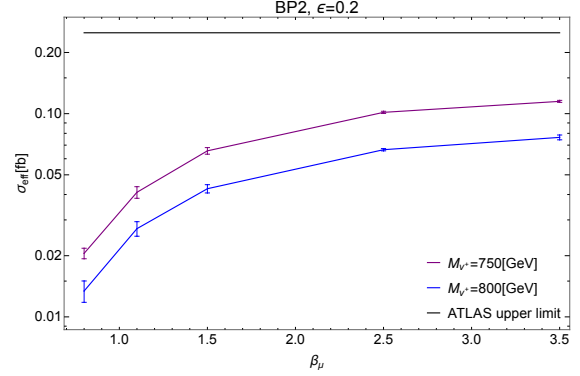
The current experimental limits for the DY production of new physics come from the search of sleptons at ATLAS [13], in a final state composed of a lepton pair (electrons and muons) and missing energy. Since we have restricted our study to the case only with muons in the final state, the generated events must satisfy the selection criteria described in Table III. As can be seen in Figures 3 and 4, the limit on the  $\beta_{\mu}$  coupling is more stringent in the low mass regime, and this limit relaxes as  $M_{V+}$  increases. Moreover, for  $M_{V+} = 800[\text{GeV}]$  the cross section is suppressed enough to escape the ATLAS upper limit, up to the perturbative scale ( $\beta \sim \sqrt{4\pi}$ ). It's worth mentioning that these conclusions are true for both benchmark points, the main difference between them is that the values of the cross section are smaller

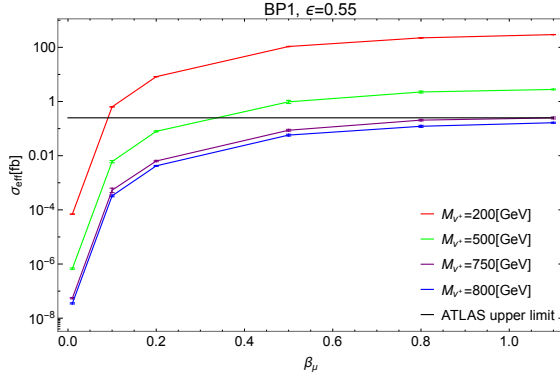
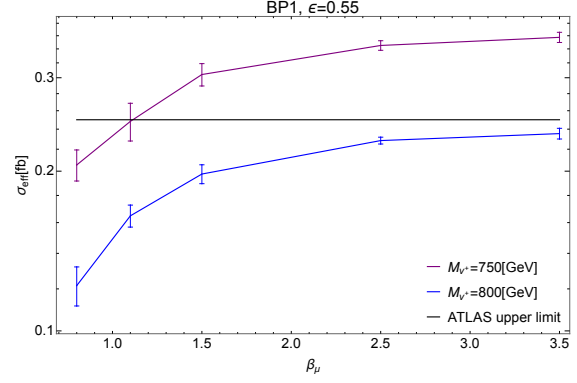
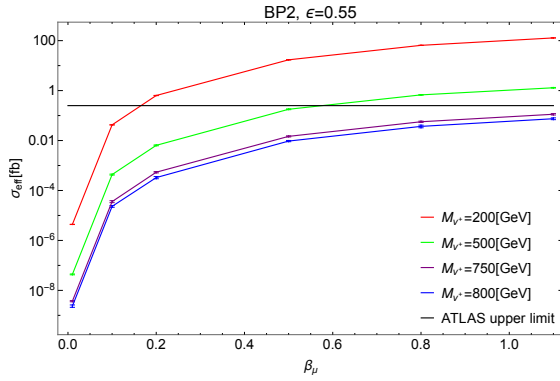
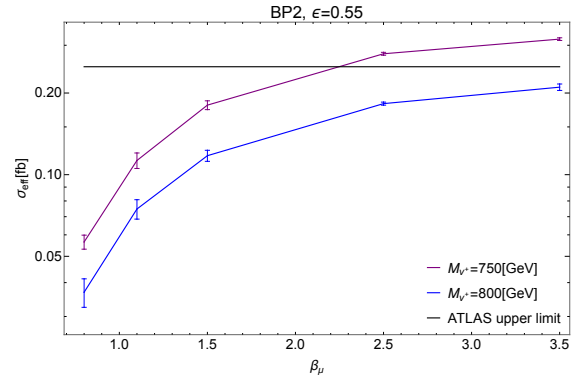
for BP2. This suppression is explained by the contribution to the charged vector decay width, which is proportional to  $|\beta_\tau|^2$ . On the other hand, we obtained the kinematical distributions for  $M_{ll}$ ,  $p_T^{miss}$ , and  $\cos\theta$ , which is defined as the angle between the outgoing leptons. The model predicts longer tails for  $M_{ll}$  and  $p_T^{miss}$ , as expected for SM extensions with heavy mediators, while the angular distribution presents a slightly distinctive pattern compared to the SM background.

object	definition	condition
$p_T(l+)$	Transverse momentum of the positively charged lepton	$> 25$ [GeV]
$p_T(l-)$	Transverse momentum of the negatively charged lepton	$> 25$ [GeV]
$\eta(l^+)$	pseudorapidity of the positively charged lepton	$< 2.7$
$\eta(l^-)$	pseudorapidity of the negatively charged lepton	$< 2.7$
$M_{ll}$	Invariant mass of the SFOS lepton pair	$\geq 121.2$ [GeV]
$p_T^{miss}$	Transverse component of the missing momentum vector	$> 110$ [GeV]

TABLE III: Event selection criteria for DY production. These cuts were taken from reference [13]



(a) BP1, low  $\beta_\mu$  values(b) BP1, high  $\beta_\mu$  values(c) BP2, low  $\beta_\mu$  values(d) BP2, high  $\beta_\mu$  valuesFIG. 3: Effective cross section for DY production, for  $\epsilon = 0.2$ .

(a) BP1, low  $\beta_\mu$  values(b) BP1, high  $\beta_\mu$  values(c) BP2, low  $\beta_\mu$  values(d) BP2, high  $\beta_\mu$  valuesFIG. 4: Effective cross section for DY production, for  $\epsilon = 0.55$ .

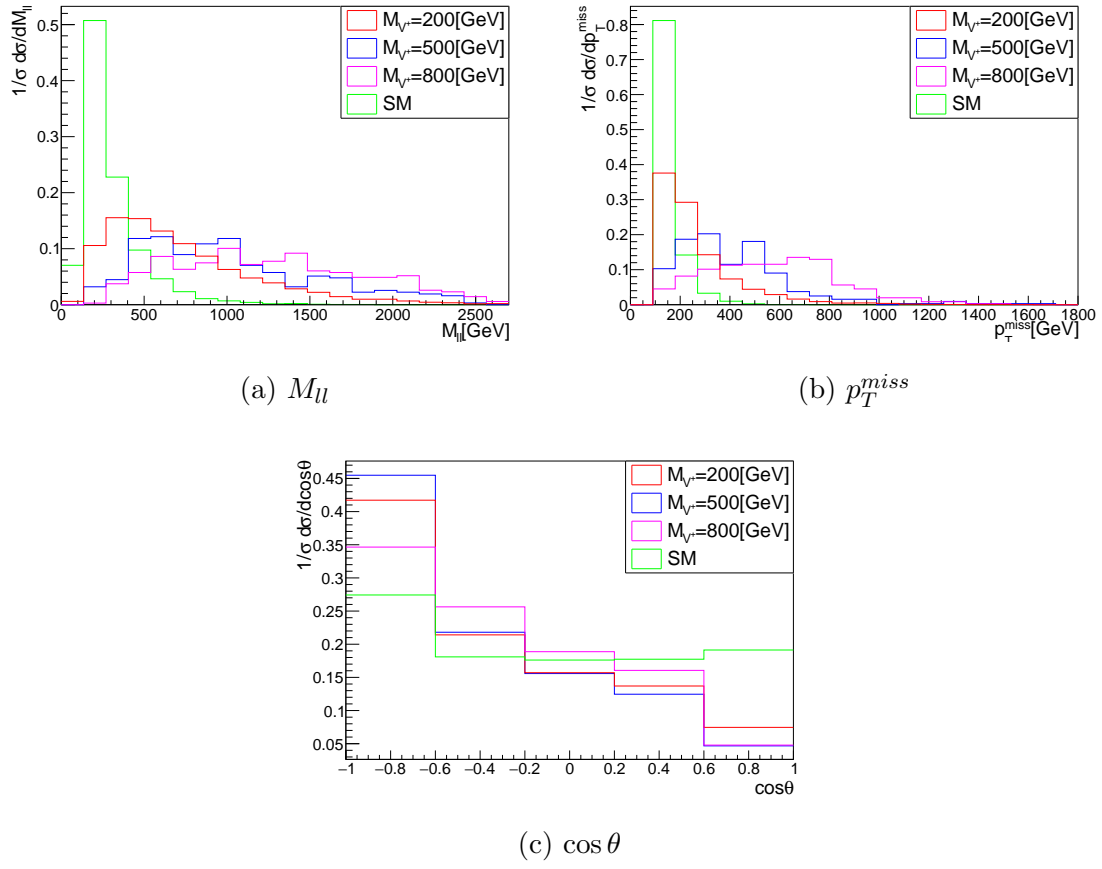


FIG. 5: Relevant kinematical distributions for DY production considering BP1 and  $\beta_{\mu} = 0.01$ .

## V. VECTOR BOSON FUSION PRODUCTION

For VBF production, the event selection criteria are shown in Table V. Due to the strong limits arising from DY production, we have computed the VBF cross section for  $M_{V^+} = 800[\text{GeV}]$  and  $\beta_\mu = 3.5$  for two benchmark points. Among the previously presented kinematical objects, we also considered the  $H_T$  variable, defined as the scalar sum of the  $p_T$  from all the outgoing jets. The effective cross sections can be seen in Table IV. While these cross sections are similar to the DY cross sections for the same parameter space points, the VBF background is significantly larger than the DY background. Indeed, taking the results from references [13, 14], we have found the following relation

$$\frac{\sigma_{bkg}^{DY}}{\sigma_{bkg}^{VBF}} \approx 0.01. \quad (9)$$

The big difference between the background cross sections makes the VBF significance considerably smaller under these conditions. The relevant kinematical distributions are depicted in Figure 6. As can be seen, the results are similar to the DY kinematics, however, the angular distribution of the lepton pair in the background sample has less overlapping with the signal. This feature of the model can be used to implement a trigger, that can help to improve the discovery prospects under this production mechanism.

	$\sigma_{eff}(\epsilon = 0.2)[\text{fb}]$	$\sigma_{eff}(\epsilon = 0.55)[\text{fb}]$
BP1	$0.0502 \pm 0.0011$	$0.138 \pm 0.003$
BP2	$0.0487 \pm 0.0007$	$0.134 \pm 0.002$

TABLE IV: Cross sections for VBF production, considering  $\beta_\mu = 3.5$  and  $M_{V^+} = 800[\text{GeV}]$ .

object	definition	condition
$p_T(l+)$	Transverse momentum of the positively charged lepton	$\geq 25$ [GeV]
$p_T(l-)$	Transverse momentum of the negatively charged lepton	$\geq 25$ [GeV]
$M_{ll}$	Invariant mass of the SFOS lepton pair	$\geq 12$ [GeV]
$p_T^{miss}$	Transverse component of the missing momentum vector	$> 200$ [GeV]
$\Delta\phi(jet_1, p_T^{miss})$	Azimuthal separation between $p_T^{miss}$ and the first jet	$\geq 0.4$
$\Delta\phi(jet_2, p_T^{miss})$	Azimuthal separation between $p_T^{miss}$ and the second jet	$\geq 0.4$

TABLE V: Event selection criteria for VBF production. These cuts were taken from reference [14]

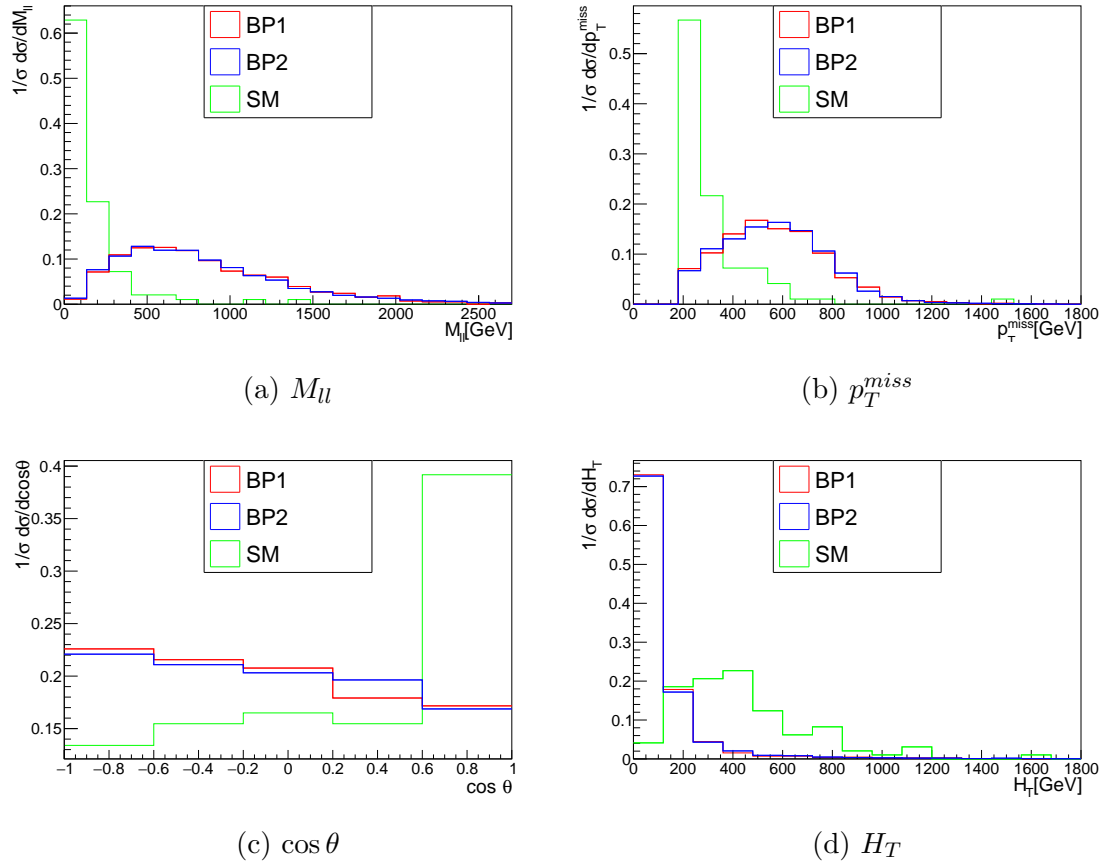


FIG. 6: Relevant kinematical distributions for VBF production considering

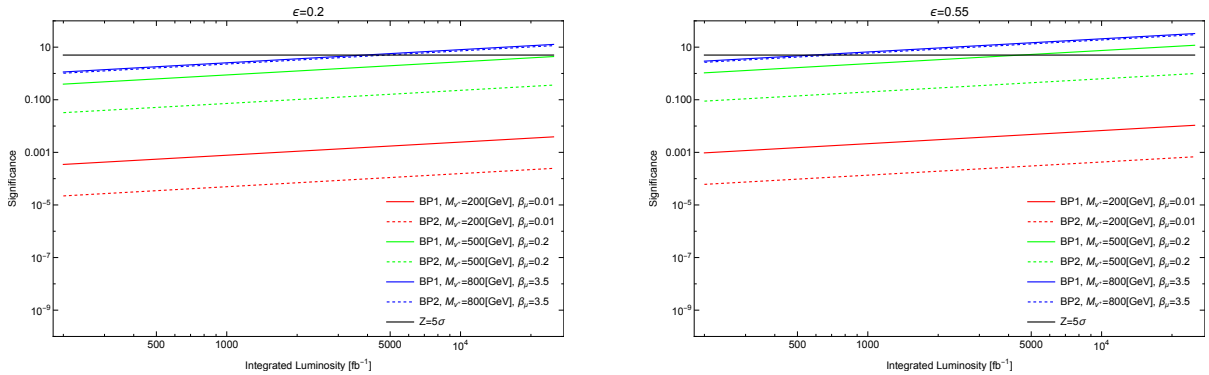
$$M_{V^+} = 800[\text{GeV}] \text{ and } \beta_\mu = 3.5.$$

## VI. PROJECTION FOR FUTURE COLLIDERS

In order to study the discovery prospects of our model, we consider some scenarios that can be studied in future experiments. For this section, we restricted ourselves to DY production. Our predictions are based on the standard definition of significance ( $Z$ )

$$Z = \frac{s}{\sqrt{s+b}}, \quad (10)$$

where  $s$  and  $b$  stands for the number of signal and background events, respectively. Firstly, we have studied scenarios with fixed value of center of mass energy ( $\sqrt{s} = 13[\text{TeV}]$ ), this choice is motivated by the fact that the background cross section could be affected by  $\sqrt{s}$ . In Figure 7, we show the  $M_{V^+} = 800[\text{GeV}]$  scenario which is the most promising for luminosities that can be reached at early stage of the HL-LHC. On the other hand, the strong suppression on the couplings at the  $M_{V^+} = 200[\text{GeV}]$  scenario makes it hard to probe in the near future, being practically undetectable during HL-LHC lifetime. It is worth to mention, that the lower mass regime ( $M_{V^+} = 200[\text{GeV}]$ ) could be probed in a scenario that consider the vector decay into tau leptons, however, this is not studied in this work.



(a)  $\epsilon = 0.2$

(b)  $\epsilon = 0.55$

FIG. 7: Significance projections for high luminosities.

In Figure 8 we show the expected number of event for  $\int L dt = 3000[\text{fb}^{-1}]$  at  $\sqrt{s} = 13[\text{TeV}]$ . The horizontal dotted lines ( $Z = 1\sigma, 3\sigma, 5\sigma$ ) stand for the number of events needed to overpass certain significance level. Our result shows that a large region of the allowed parameter space, all the points above  $Z = 5\sigma$ , can be probed during the HL-LHC lifetime

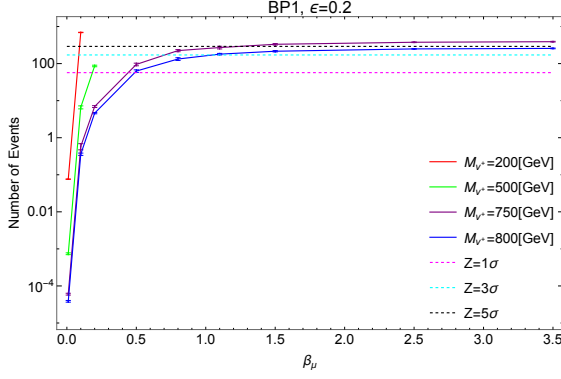
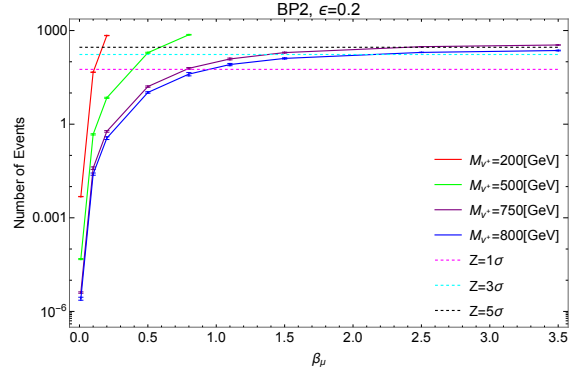
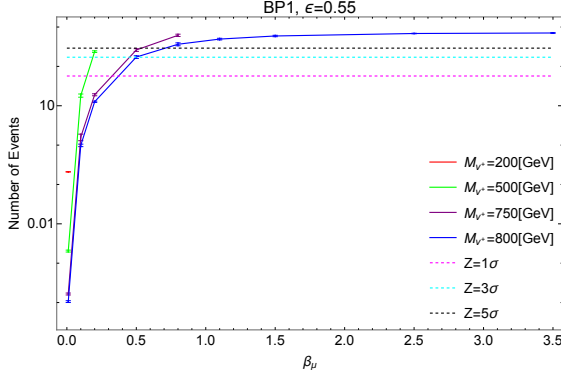
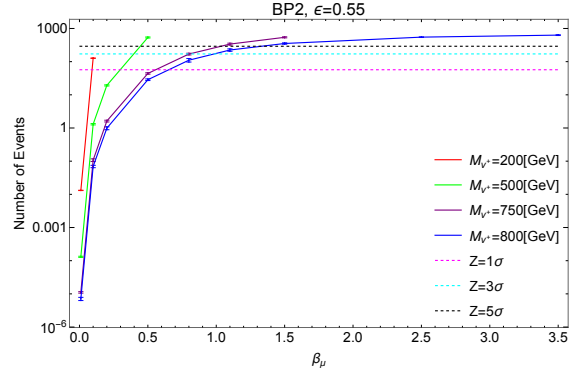
(a) BP1,  $\epsilon = 0.2$ (b) BP2,  $\epsilon = 0.2$ (c) BP1,  $\epsilon = 0.55$ (d) BP2,  $\epsilon = 0.55$ 

FIG. 8: Expected number of events for  $\int L dt = 3000[\text{fb}^{-1}]$  at  $\sqrt{s} = 13[\text{TeV}]$ . The horizontal dotted lines stand for the number of events needed to overpass the corresponding significance level

## VII. LOWER LIMITS

Depending on the model kinematical regime, some constraints on the couplings of the HNL can be obtained from astrophysical observations. For instance, when the HNL is a DM candidate, we can use the DM abundance measured by Planck [1] as input to set limits.

According to reference [6] the annihilation cross section for the left handed HNL has the following form

$$\langle \sigma v \rangle = \sum_{k,k'=\{e,\mu,\tau\}} |\beta_k^* \beta_{k'}|^2 \frac{M_N^2}{8\pi} \left( 1 + \frac{8T_f}{M_N} \right) \left( \frac{1}{M_{V^+}^4} + \frac{4}{(M_{V^1}^2 + M_{V^2}^2)^2} \right). \quad (11)$$

In order to avoid overabundance, the thermally averaged cross section must satisfy the

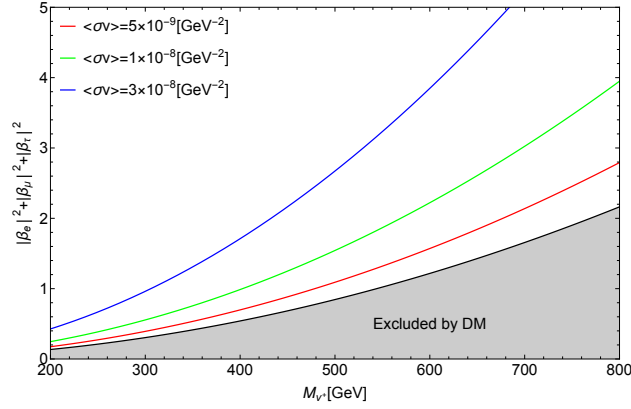


FIG. 9: Allowed parameter space considering the DM constraint.

following lower bound (for instance, see references [15–17]):

$$\langle\sigma v\rangle \geq 3 \times 10^{-9} [\text{GeV}^{-2}], \quad (12)$$

which provides a restriction for the parameter space as seen in Figure 9.

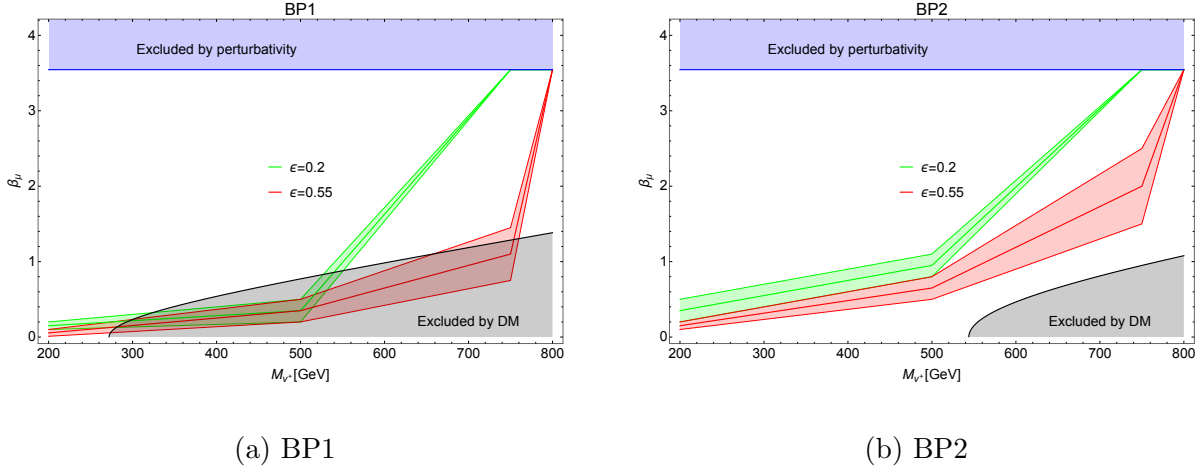


FIG. 10: Combined limits on the parameter space.

The collider limits presented in this work can be combined with the DM limits, as is shown in Figure 10, there is an interesting interplay between the upper limits from ATLAS and the lower limit from dark matter. Due to this interplay, a large part of the parameter space in BP1 seems to be excluded by dark matter abundance, however, it's worth emphasizing that the lower limit is a rough approximation and a rigorous study on dark matter relic



abundance can help to precisely rule out that part of the parameter space (the grey region in Figure 10).

## VIII. CONCLUSIONS

In this work, we have studied a simplified extension of the SM based on a Massive Vector Doublet and a Left-Handed HNL. The results have shown that the model produces a characteristic signal composed by a SFOS lepton pair and missing energy. While this state has been studied in the past, our analysis shows that the angular distribution of the lepton pair is a key variable for the identification of new physics in this final state. Indeed, it may constitute a discovery method in future experiments. Moreover, the kinematical analysis presented in this work could be repeated for different BSM scenarios related to this final state, and the angular distributions could be useful to classify different models. We have performed an analysis to set limits on the parameter space using experimental cuts applied by current searches of new physics and considering two different prescriptions for the detector efficiency:  $\epsilon = 0.2$  and  $\epsilon = 0.55$ . The first is well motivated by the simulation of the detector response and the latter is an optimistic prediction considering future developments of the LHC. The main effect of the efficiency is reflected in the definition of upper limits on the parameter space, these limits get relaxed for the lower efficiency. However, the remaining parameter space can be probed at the HL-LHC in both prescriptions.

On the other hand, we have constrained the parameter space based on the dark matter relic abundance. The lower bound depends strongly on the exotic neutrino coupling to the three families of leptons, however, we restricted our analysis only to the coupling to muons. One possible way to constrain all flavors is to consider Lepton Flavor Violation (LFV) processes. These type of processes can be suited in the model at 1 loop, but the calculation of these loops is not trivial, due to the non minimal gauge couplings. Therefore, a rigorous study of the radiative processes will be carried out in a future work.

## Appendix A: Analysis validation

In order to check the consistency of our analysis, we validated our result with a full simulation using pythia 8.2, fastjet 3.3.4 and Delphes 3.5.0 [18–20], the latter one interfaced

with MadAnalysis 5 [21–29] for recasting previous results from ATLAS. In particular, we considered the implementation of Ref. [13] that is publicly available in the MadAnalysis 5 Public Analysis Database [30]. We focused on DY production and BP1. As can be seen from Figure 11, the conservative choice of the efficiency shows a stronger concordance with the efficiencies obtained with MadAnalysis, however, considering a larger efficiency is helpful for future searches, considering the development of detector technology that will be implemented in future stages of the LHC. Therefore, we show our results considering both prescriptions for the detector efficiency.

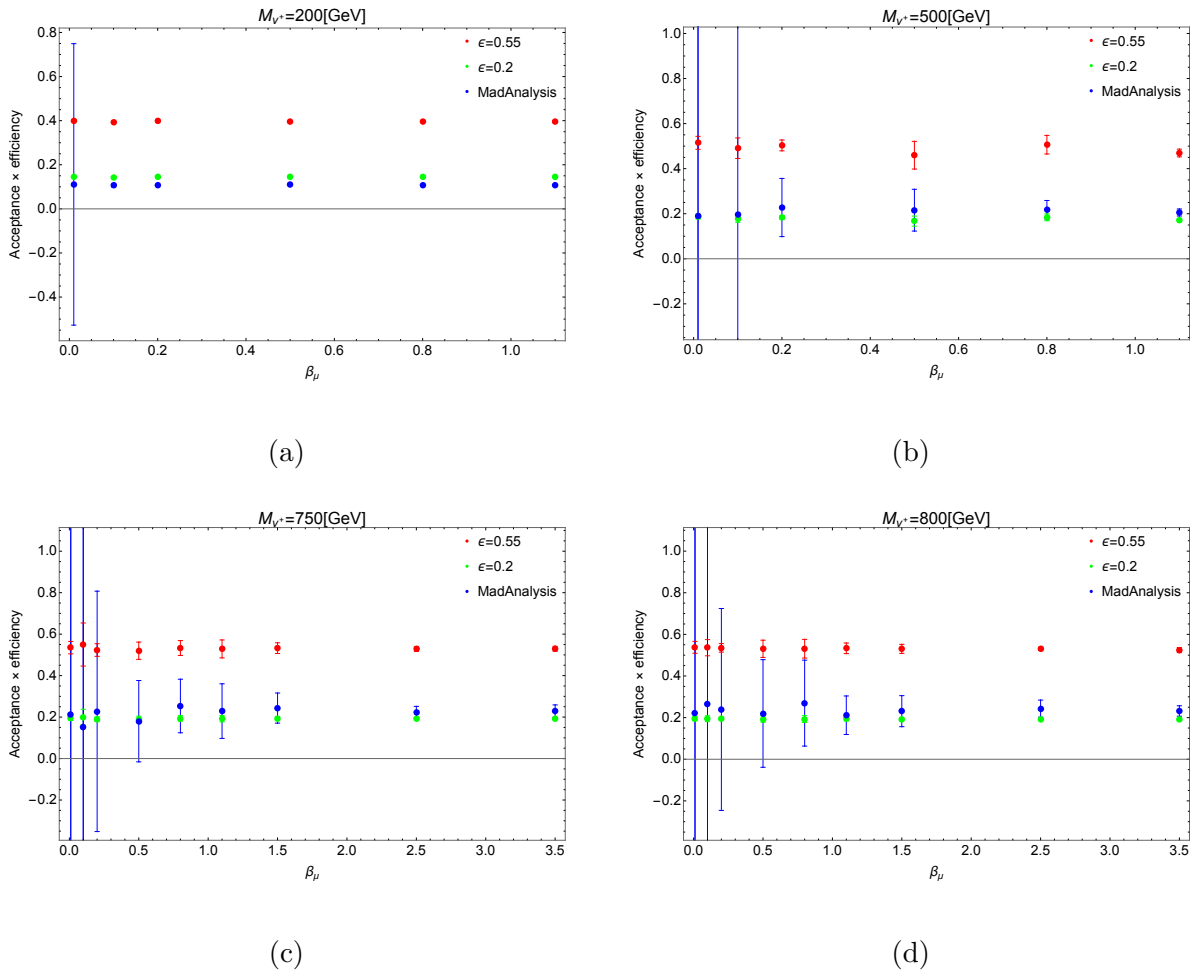


FIG. 11: Efficiency comparison between our cut-flow and the result obtained with MadAnalysis

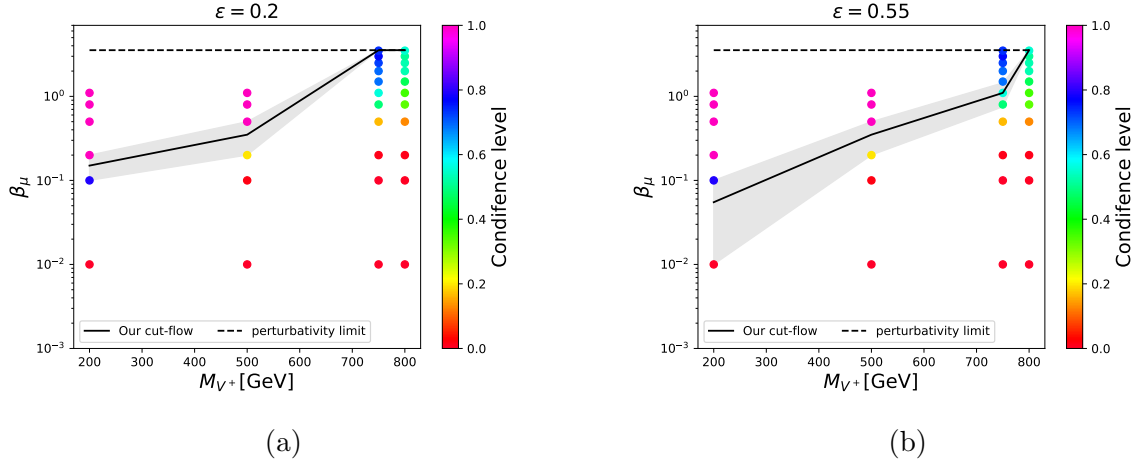


FIG. 12: Comparison between the exclusion limits obtained from different methods.

## ACKNOWLEDGEMENTS

This work was funded by ANID - Millennium Program - ICN2019\_044. Also, we would like to thank to the DGIIP-UTFSM for funding during the development of this work. AZ was partially supported by Proyecto ANID PIA/APOYO AFB220004 (Chile) and Fondecyt 1230110.

- 
- [1] **Planck** Collaboration, P. A. R. Ade *et al.*, “Planck 2015 results. XIII. Cosmological parameters,” *Astron. Astrophys.* **594** (2016) A13, [arXiv:1502.01589 \[astro-ph.CO\]](#).
  - [2] M. Cirelli, N. Fornengo, and A. Strumia, “Minimal dark matter,” *Nucl. Phys. B* **753** (2006) 178–194, [arXiv:hep-ph/0512090](#).
  - [3] A. Belyaev, G. Cacciapaglia, J. McKay, D. Marin, and A. R. Zerwekh, “Minimal Spin-one Isotriplet Dark Matter,” *Phys. Rev. D* **99** no. 11, (2019) 115003, [arXiv:1808.10464 \[hep-ph\]](#).
  - [4] B. D. Sáez, F. Rojas-Abatte, and A. R. Zerwekh, “Dark Matter from a Vector Field in the Fundamental Representation of  $SU(2)_L$ ,” *Phys. Rev. D* **99** no. 7, (2019) 075026, [arXiv:1810.06375 \[hep-ph\]](#).
  - [5] A. E. Cárcamo Hernández, J. Vignatti, and A. Zerwekh, “Generating lepton masses and mixings with a heavy vector doublet,” *J. Phys. G* **46** no. 11, (2019) 115007,

- arXiv:1807.05321 [hep-ph].
- [6] P. Van Dong, D. Van Loi, L. D. Thien, and P. N. Thu, “Novel imprint of a vector doublet,” *Phys. Rev. D* **104** no. 3, (2021) 035001, arXiv:2104.12160 [hep-ph].
  - [7] E. Ma, “Verifiable radiative seesaw mechanism of neutrino mass and dark matter,” *Phys. Rev. D* **73** (2006) 077301, arXiv:hep-ph/0601225.
  - [8] N. D. Christensen and C. Duhr, “FeynRules – feynman rules made easy,” *Computer Physics Communications* **180** no. 9, (Sep, 2009) 1614–1641.  
<https://doi.org/10.1016%2Fj.cpc.2009.02.018>.
  - [9] A. Alloul, N. D. Christensen, C. Degrande, C. Duhr, and B. Fuks, “FeynRules 2.0 — a complete toolbox for tree-level phenomenology,” *Computer Physics Communications* **185** no. 8, (Aug, 2014) 2250–2300. <https://doi.org/10.1016%2Fj.cpc.2014.04.012>.
  - [10] C. Degrande, C. Duhr, B. Fuks, D. Grellscheid, O. Mattelaer, and T. Reiter, “UFO – the universal FeynRules output,” *Computer Physics Communications* **183** no. 6, (Jun, 2012) 1201–1214. <https://doi.org/10.1016%2Fj.cpc.2012.01.022>.
  - [11] J. Alwall, R. Frederix, S. Frixione, V. Hirschi, F. Maltoni, O. Mattelaer, H.-S. Shao, T. Stelzer, P. Torrielli, and M. Zaro, “The automated computation of tree-level and next-to-leading order differential cross sections, and their matching to parton shower simulations,” *Journal of High Energy Physics* **2014** no. 7, (Jul, 2014) .  
<https://doi.org/10.1007%2Fjhep07%282014%29079>.
  - [12] **ATLAS** Collaboration, G. Aad *et al.*, “Muon reconstruction and identification efficiency in ATLAS using the full Run 2  $pp$  collision data set at  $\sqrt{s} = 13$  TeV,” *Eur. Phys. J. C* **81** no. 7, (2021) 578, arXiv:2012.00578 [hep-ex].
  - [13] **ATLAS** Collaboration, G. Aad *et al.*, “Search for electroweak production of charginos and sleptons decaying into final states with two leptons and missing transverse momentum in  $\sqrt{s} = 13$  TeV  $pp$  collisions using the ATLAS detector,” *Eur. Phys. J. C* **80** no. 2, (2020) 123, arXiv:1908.08215 [hep-ex].
  - [14] **ATLAS** Collaboration, M. Aaboud *et al.*, “Search for new phenomena in events containing a same-flavour opposite-sign dilepton pair, jets, and large missing transverse momentum in  $\sqrt{s} = 13$   $pp$  collisions with the ATLAS detector,” *Eur. Phys. J. C* **77** no. 3, (2017) 144, arXiv:1611.05791 [hep-ex].
  - [15] P. Langacker, “The standard model and beyond,” 2017.

- [16] **Particle Data Group** Collaboration, R. L. Workman *et al.*, “Review of Particle Physics,” *PTEP* **2022** (2022) 083C01.
- [17] S. Profumo, L. Giani, and O. F. Piattella, “An Introduction to Particle Dark Matter,” *Universe* **5** no. 10, (2019) 213, [arXiv:1910.05610 \[hep-ph\]](#).
- [18] T. Sjöstrand, S. Ask, J. R. Christiansen, R. Corke, N. Desai, P. Ilten, S. Mrenna, S. Prestel, C. O. Rasmussen, and P. Z. Skands, “An introduction to PYTHIA 8.2” *Comput. Phys. Commun.* **191** (2015) 159–177, [arXiv:1410.3012 \[hep-ph\]](#).
- [19] M. Cacciari, G. P. Salam, and G. Soyez, “FastJet User Manual,” *Eur. Phys. J. C* **72** (2012) 1896, [arXiv:1111.6097 \[hep-ph\]](#).
- [20] **DELPHES 3** Collaboration, J. de Favereau, C. Delaere, P. Demin, A. Giammanco, V. Lemaître, A. Mertens, and M. Selvaggi, “DELPHES 3, A modular framework for fast simulation of a generic collider experiment,” *JHEP* **02** (2014) 057, [arXiv:1307.6346 \[hep-ex\]](#).
- [21] J. Y. Araz, A. Buckley, and B. Fuks, “Searches for new physics with boosted top quarks in the MadAnalysis 5 and Rivet frameworks,” [arXiv:2303.03427 \[hep-ph\]](#).
- [22] G. Alguero, J. Y. Araz, B. Fuks, and S. Kraml, “Signal region combination with full and simplified likelihoods in MadAnalysis 5,” *SciPost Phys.* **14** (2023) 009.  
<https://scipost.org/10.21468/SciPostPhys.14.1.009>.
- [23] J. Y. Araz, B. Fuks, M. D. Goodsell, and M. Utsch, “Recasting LHC searches for long-lived particles with MadAnalysis 5,” *Eur. Phys. J. C* **82** no. 7, (2022) 597, [arXiv:2112.05163 \[hep-ph\]](#).
- [24] J. Y. Araz, B. Fuks, and G. Polykratis, “Simplified fast detector simulation in MADANALYSIS 5,” *Eur. Phys. J. C* **81** no. 4, (2021) 329, [arXiv:2006.09387 \[hep-ph\]](#).
- [25] J. Y. Araz, M. Frank, and B. Fuks, “Reinterpreting the results of the LHC with MadAnalysis 5: uncertainties and higher-luminosity estimates,” *Eur. Phys. J. C* **80** no. 6, (2020) 531, [arXiv:1910.11418 \[hep-ph\]](#).
- [26] E. Conte and B. Fuks, “Confronting new physics theories to LHC data with MADANALYSIS 5,” *Int. J. Mod. Phys. A* **33** no. 28, (2018) 1830027, [arXiv:1808.00480 \[hep-ph\]](#).
- [27] B. Dumont, B. Fuks, S. Kraml, S. Bein, G. Chalons, E. Conte, S. Kulkarni, D. Sengupta, and C. Wymant, “Toward a public analysis database for LHC new physics searches using MADANALYSIS 5,” *Eur. Phys. J. C* **75** no. 2, (2015) 56, [arXiv:1407.3278 \[hep-ph\]](#).

- [28] E. Conte, B. Dumont, B. Fuks, and C. Wymant, “Designing and recasting LHC analyses with MadAnalysis 5,” *Eur. Phys. J. C* **74** no. 10, (2014) 3103, [arXiv:1405.3982 \[hep-ph\]](#).
- [29] E. Conte, B. Fuks, and G. Serret, “MadAnalysis 5, A User-Friendly Framework for Collider Phenomenology,” *Comput. Phys. Commun.* **184** (2013) 222–256, [arXiv:1206.1599 \[hep-ph\]](#).
- [30] B. Fuks and J. Y. Araz, “Implementation of a search for sleptons and electroweakinos in the dilepton + MET channel (139 fb-1; ATLAS-SUSY-2018-32),” 2020.  
<https://doi.org/10.14428/DVN/EA4S4D>.